Performance testing of a long-strip two-end readout multi-gap resistive plate chamber*

WANG Xiao-Bin(王小斌) WANG Yi(王义)1) LUO Ming(罗明)
LI Yuan-Jing(李元景) CHENG Jian-Ping(程建平)

(Department of Engineering Physics, Tsinghua University, Beijing 100084, China)

Abstract Multi-gap Resistive Plate Chamber (MRPC) is a new generation of gas detector with good timing and spacial resolution, whose technique is widely applied in some recent high energy (nuclear) physics experiments. In this letter, we report a long-strip two-end readout MRPC and its test beam performance. The measurements show that the long-strip performs a transmission line characteristic and the impedance is independent of the length of strip. The MRPC module we developed is presented to gain a timing resolution of ~80 ps and a spacial resolution of ~6.4 mm. The possible application of the MRPC is also discussed.

Key words MRPC, timing resolution, spacial resolution

PACS 25.40.Cm, 28.75.Gz, 21.60.-n

1 Introduction

Due to the characteristics of high detecting efficiency (~ 95%), good timing resolution (~100 ps), stable working capability and low costs, Muti-gap Resistive Plate Chamber (MRPC) tends to be widely used in the area of high energy physics experiments. For example, the technique was applied to compose a large area Time-Of-Flight (TOF) detector at STAR[1] and another at the ALICE experiment[2] of LHC. The MRPC module produced for STAR TOF program has 6 pads and each pad has a geometrical size of 31 mm×63 mm. It is reported that with the TOF detector, STAR can provide good particle identification capabilities at mid-to-high transverse momentum range, which covers kaon/pion up to ~ 1.6 GeV/c and proton/kaon up to ~ 3 GeV/c[3].

In this letter, we report a long-strip and large area (855 mm×255 mm) MRPC and its beam testing performance. The large area will effectively reduce the number of readout channels and the corresponding electronic costs. The technique can be applied to a low particle flux environment. One of possible applications of the long MRPC module is, covering out of the STAR magnet and performing as a mid-rapidity muon telescope detector system[4, 5]. In this case, particles like electrons (kaons) are absorbed (in part) by the magnet iron material and, the counting rate capability by a long-strip MRPC can satisfy the particle densities[6]. The detections to these muons may reveal more related physics topics, for example J/ψ or open charm spectrum via the measurements of their decay to di-muon channels[7], quarkonia production and the Drell-Yan process in heavy ion collisions[8].

For the purposes of these applications, we researched and developed a long-strip two-end readout MRPC, whose readout strip performs a transmission line and an impedance characteristics. The readout amplitudes of the two ends at a fired strip are the same and independent of the charged particle incident position. At the same time, the position can be obtained by the timing difference from the two ends of the strip. The test beam results show that the timing resolution of the MRPC module is ~ 80 ps and the spacial resolution is ~ 6.4 mm.

2 Detector structure

Figure 1 shows the detector structure and its

Received 6 May 2008, Revised 4 June 2008
* Supported by NSFC (10620120287, 10610285, 10675072, 10775082)
1) E-mail: yiwang@mail.tsinghua.edu.cn

geometry of a MRPC module. The detector body covers an area of 855 mm×255 mm and is composed by two stacks of chambers. Each chamber is a six gas-gaps long-strip MRPC individually, in which the gas-gap is 0.22 mm. Such a narrow gas-gap can provide good response timing capabilities. The thickness of an inner glass which is used to form the gas-gap is 0.5 mm. The volume resistivity of the glass is 10^{12}—10^{13} Ω·cm. In a single chamber, two outer glass plates (thickness 0.7 mm) are coated by permanent static dissipative anti-static coatings and used as high-voltage electrodes, with the surface resistivity of 10 MΩ/□. The six strips of a chamber distribute equably with a distance of 5 mm between one strip and another. The geometric size of a strip is 850 mm×30 mm, which is shown in Fig. 2.

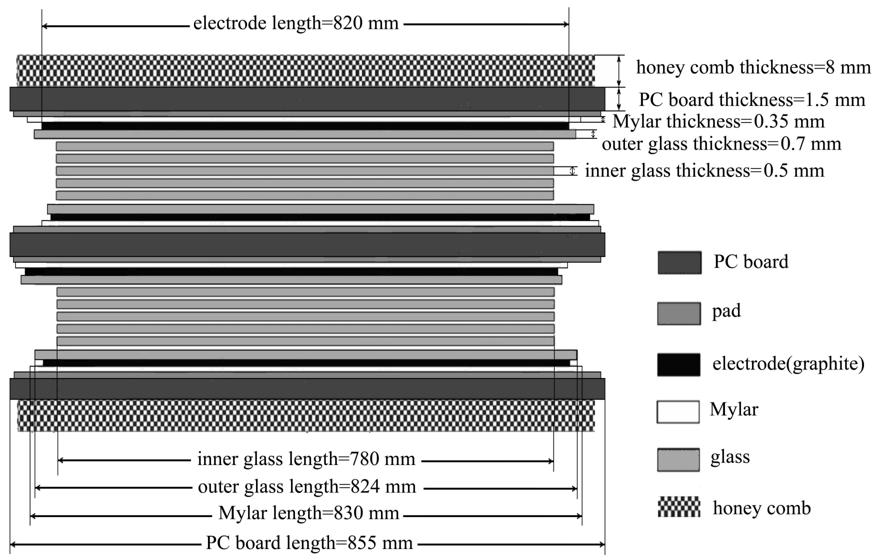

Fig. 1. The structure of the detector and its geometry. The detector body is composed of two stacks of MRPC. Each chamber (stack) has six gas-gaps which are shaped between two layers of floating glass. The electrode pads are outer glass coated by permanent static dissipative anti-static coatings.

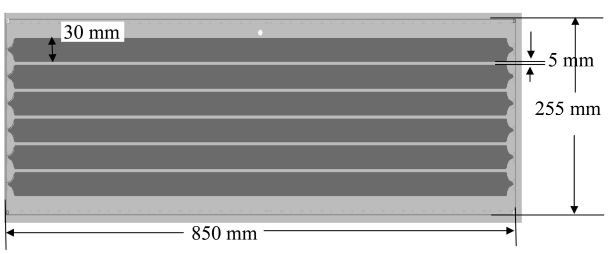

Fig. 2. The geometry of a readout strip. The six strips distribute equably on a PC board.

The working gas of the module is mixed by Freon (95%) and Isobutane (5%)[9]. When the two electrodes which are close to the middle PC board are applied with negative high-voltage and the other two are applied with positive, a thus generated electric field intensity can reach a scale of 10^4—10^5 V/cm in the gas-gaps[10]. The field can yield immediate avalanche amplification of initial ionization produced in the detective working gas by a charged particle. The floating inner glass functions as floating electrodes to collect induced charge generated in the gaps. The induced signals are read out at the two ends of the fired strip. At each end, the total signal is summed from the corresponding strips from the upper and the lower chambers and sent to a FEE board. The timing difference of a signal reaching at two ends can be used to calculate the charged particle incident position.

3 Experiment layout

We used the test beam facility at Fermi National Accelerator Laboratory (FNAL) to measure the detection efficiency, the timing resolution and the spacial resolution of the MRPC module. Fig. 3 shows the detectors layout in the experiment (T963). Three pieces of scintillator are used as Time-Of-Flight (TOF) detectors to record the start time of an incident particle. Five pieces of Multi-wire Proportional Chambers (WMPC) are positioned along the beam line to reconstruct the particle track. Between the MRPC module and the TOF_2, three Gas Electron Multiplier (GEM)[11] detectors are placed to measure the particle incident position. The beam energy can

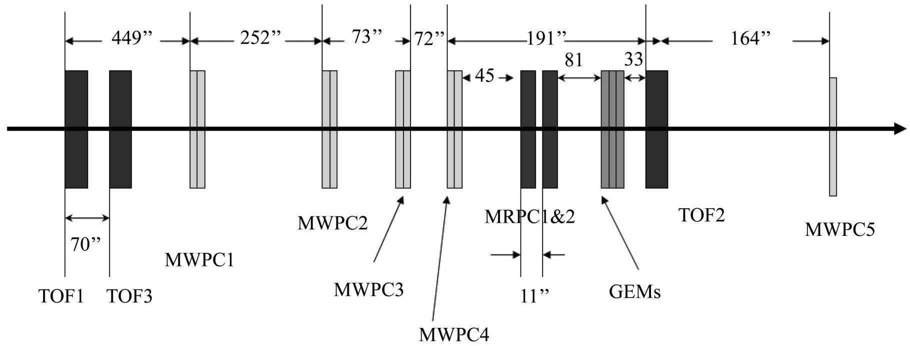

Fig. 3. The detectors layout in the test beam facility at FNAL. The middle arrow in the plot shows the beam direction.

be fixed in a certain value within the range of 1—120 GeV, in which the particle type can be electrons, muons, pions or protons. The particle flux from the beam operating facility can be adjusted from 1 Hz to 700 Hz. The beam profile near the MRPC location is about 10 cm×10 cm. In the experiment, the trigger signal is provided by coincidence logic from the three TOF detectors. The $T_{\rm start}$ signal is provided by $\rm TOF_1$, while the reference time $T_{\rm ref}$ is from $\rm TOF_2$ + $\rm TOF_3$.

4 Results

The long-strip performs a transmission line characteristics and the impedance is independent of the length of strip. In Fig. 4, ADC1 and ADC2 are the amplitudes from the two ADC readouts of a fired strip. The measurements show that the two values from an event are well correlated and equal. This indicates that the output amplitudes of a particle response at the ends are independent of its incident position on the strip.

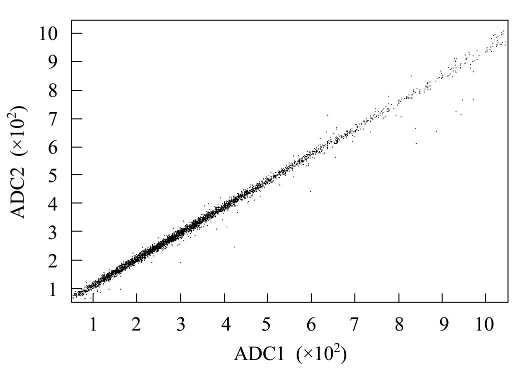

Fig. 4. Correlation of the amplitudes from the two ADC readouts of a strip.

The performance of good timing resolutions and high detective efficiency[12] are required when MRPCs are applied to compose a Time-of-Flight detector[13]. Fig. 5 shows the efficiency plateau (the upper panel) and the timing resolution (the lower one) as a function of electric field generated by high voltage. The results present a fact that, when the electric field strength raised to 106 kV/cm and above, the detective efficiency $\geqslant 90\%$ and the timing resolution ~80 ps are obtained. These features will be helpful in terms of precise particle identification. The method to calculate timing resolution is, to take the average value of $T_{\rm TOF2}$ and $T_{\rm TOF3}$ as a reference time and count the σ value of the distribution of average flight time from the two ends after the time-slewing correction.

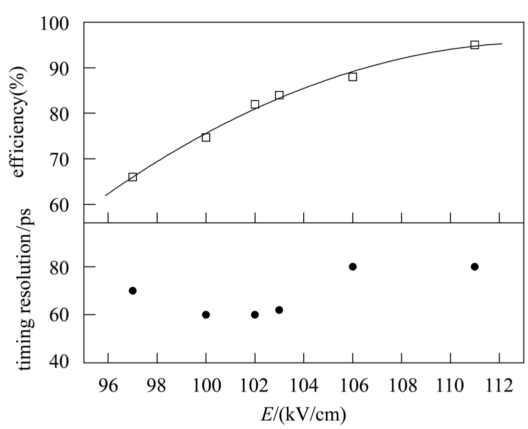

Fig. 5. The detective efficiency plateau (upper) and the timing resolution (lower) as a function of electric field for the MPRC module.

The GEM detectors track particles and provide their (X, Y) positions at the MRPC plates. Fig. 6 shows a linear behavior between the timing difference of a fired strip and the corresponding charged particle positions detected by GEM which has a spacial resolution < 0.01 cm. The distribution tells a truth that the long-strip performs a characteristic of transmission line and the module can be applied as a position sensitive detector.

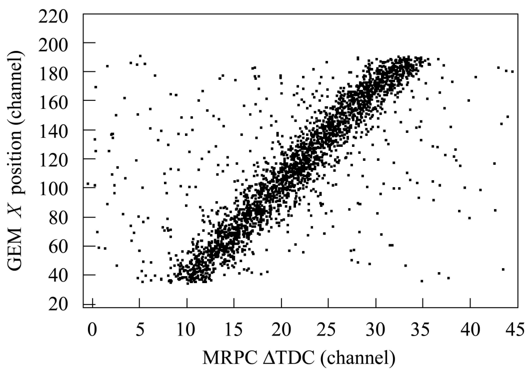

Fig. 6. A linear behavior between the timing difference from the two ends of a fired strip and the corresponding particle position measured by GEM detector. The strip is in X (horizontal) direction. The units of the plot axises are TDC channel and GEM channel respectively.

Since one TDC count corresponds to 50 ps, the position difference measured by MRPC module and GEM can be obtained from Eq. (1).

$$\Delta X = \frac{50(\text{ps/ch}) \times \Delta\text{TDC}}{2 \times 60(\text{ps/cm})} - X_{\text{GEM}} \ . \tag{1}$$

In the equation, 60 ps/cm is the signal transmitting speed, ΔTDC is the timing difference from the two readouts of the fired strip, and X_{GEM} is the position reconstructed by GEM. Fig. 7 shows that the MRPC module has a spacial resolution of ~6.4 mm.

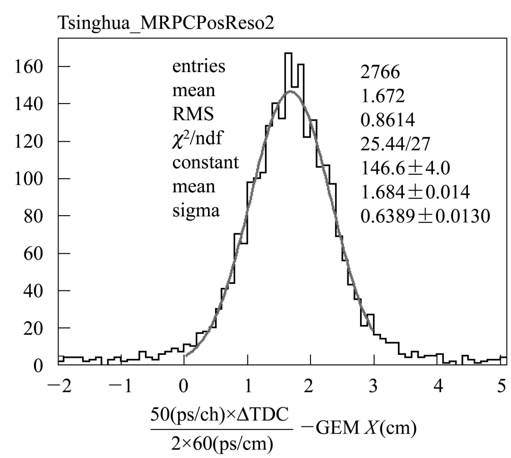

Fig. 7. The spacial resolution of the MRPC module is obtained from a Gaussian fit to the ΔX distribution of the data sample. The value of σ parameter from the Gaussian distribution is ~6.4 mm. The reference particle positions are provided by the GEM detectors.

We have tested the particle identification capability of the MRPC module from the experiment as well, since the beam contains both protons and mesons (π and μ). This could help us to understand the reliability of the PID performance via real particle runs. Fig. 8 shows the time of flight measured by the MRPC and scintillators at the beam energy 4 GeV. In the plot, the X axis is the measured time of flight, which can be obtained from Eq. (2).

$$\Delta T = (T_1 + T_2) - (T_{\text{TOF2}} + T_{\text{TOF3}}). \tag{2}$$

The factor of T_1 (T_2) is the TDC value at one (the other) end of the investigated MRPC strip. The values of $T_{\text{TOF2}} + T_{\text{TOF3}}$ are the reference time obtained by the scintillator detectors (see Fig. 3). The distance from the scintillators to the long-strip MRPCs is several meters, which scenario is equivalent to (or slightly larger than) a thickness of iron magnet yoke plus the spaces between detectors.

The result shows that, the protons distribute at far side because their heavier masses, and the peak is clearly separated from that of the mesons. The mean flight time difference between protons and mesons is about 2.5 ns (50 TDC channels) at the beam energy. Note, in the plot, these times of flight are obtained before time-slewing correction. This can help to prove that, the good timing resolution does contribute to particle quick identification in the similar environment of the particle density and the flight distance, even without other detectors.

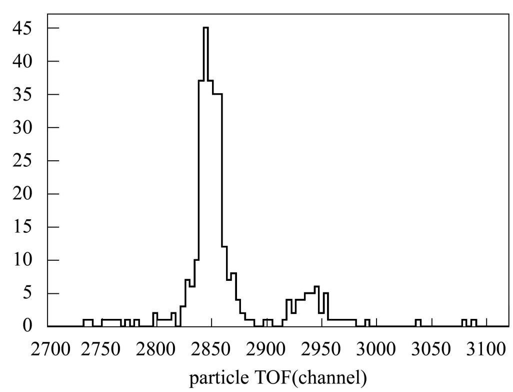

Fig. 8. The time of flight measured by the MRPC module can be used to identify protons and mesons. The right peak near 2950 (TDC channel) is formed by protons. The mesons distribute in the left peak due to lighter masses. The MRPC flight time is before time-slewing correction.

5 Summary and discussion

We report a long-strip two-end readout MRPC and its beam testing results. The module has six strips and a large-area geometry size 855 mm×

255 mm. At FNAL, we carried out the T963 experiment to test the performance of the module and proved that, a timing resolution of ~80 ps and a spacial resolution of ~6.4 mm can be obtained. The measurements also show that the long-strip performs a transmission line characteristic and the impedance is independent of the length of strip.

The particle identification capability of the MRPC module was tested via the T963 experiment. The result shows that using the particle flight time measured by the MRPC, protons in the beam can be easily identified from mesons. This would be helpful to identify particles based on timing resolution from the MRPC detector with large module, long strips and fast electronics for online trigger. Especially, for those high energy physics experiments which are equipped with thick iron magnet yokes, hadrons and electromagnetic particles can be therefore absorbed by the materials. In this case, the long-strip MRPC will be a good candidate as a compact muon detector, which serves excellent timing resolution (< 100 ps), good spatial points for tracking (< 1 cm) and some dE/dx capability at low particle flux rate environments. The advantage of low costs due to large area per readout channel will be an important factor to the large-scale application as well.

We thank Brookheaven National Lab (BNL), the Meson Test Beam Facility at FNAL, the NUCTECH Co. Ltd. and their support during the research. The authors also thank Zhangbu Xu, Lijuan Ruan, Guoji Lin, Richard Majka, Nikolai Smirnov, Frank Simon, Bernd Surrow and Erik Ramberg for their efforts at the T963 experiment and their helpful discussions.

References

1 The STAR TOF Collaboration. Proposal for a Large Area Time of Flight System for STAR

2 Akindinov A N et al. Nucl. Instrum. Methods A, 2004, **533**: 74—78

3 WU J et al. Nucl. Instrum. Methods A, 2005, **538**: 243—248

4 XU Z. A Novel and Compact Muon Telescope Detector for QCDLab, BNL LDRD Project

5 LIN G (for the STAR Collaboration). A New Large-Area Muon Telescope Detector at Mid-rapidity at RHIC, APS Annual Meeting. Oct. 27, 2006, Nashville, Tennessee

6 RUAN L (for the STAR Collaboration). QM2008 poster contribution

7 ZHANG Y (for the STAR Collaboration). J. Phys. G: Nucl. Part. Phys., 2006, **32**: S529—S532

8 RUAN L (for the STAR Collaboration). Prototype Performance of Novel Muon Detector at STAR, WWND2008. Apr. 10, 2008, South Padre Island, Texas

9 JIA Huai-Mao et al. HEP & NP, 2006, **30**(03): 232—237 (in Chinese)

10 WANG Y et al. Nucl. Instrum. Methods A, 2005, **538**: 425—430

11 Sauli F. Nucl. Instrum. Methods A, 1997, **386**: 531

12 WANG Y, WANG X. Int. J. Mod. Phys. E, 2007, **16**: 2541—2548

13 SHAO M et al. Nucl. Instrum. Methods A, 2006, **558**: 419—429